International Journal of Control and Automation
Vol.10, No.4 (2017), pp.71-84
http://dx.doi.org/10.14257/ijca.2017.10.4.07

Motion Simulation Table Control Using Improved ZPETC Approach

Rana Javed Masood[1], Dao Bo Wang[1], Muhammad Aamir[2] and Zain Anwar Ali[1]

[1]*College of Automation, Nanjing university of Aeronautics and Astronautics Nanjing, China*
[2]*Electronic Engineering Department, Sir Syed University of Engineering & Technology, Karachi, Pakistan*
rjmasood786@gmail.com, dbwangpe@nuaa.edu.cn, muaamir5@yahoo.com, zainanwar86@hotmail.com

Abstract

The conventional feed forward controller design method for motion simulation could cause the unstable tracking control because of the phase and gain error that affected by Non-minimum phase (NMP). Thus, improved zero phase error tracking controller (ZPETC) approach is introduced to overcome NMP zero problem. After introducing the basic components of the servo system, load model systems established for motor simulation of motion simulator table and proposes an improved ZPETC. Finally, the actual motion simulator turntable system is successfully applied the approximate ZPETC and improved ZPETC, and the test results were compared and analyzed. Based on the theoretical and simulation analysis, the actual motion simulator turntable successfully implemented. Improved approximation ZPETC broaden the bandwidth of the system and satisfy the required performance of the system. The simulation results of the proposed algorithm satisfy the overall tracking performance of the motion simulation turntable.

Keywords*: zero phase error tracking controller (ZPETC), Non-minimum phase (NMP), Feed-forward control, Feed-back control*

1. Introduction

The Motion simulation table control plays a very important role in the development of the aircraft, which is the key hardware device for the hardware-in-the-loop simulation and testbed in the files aeronautics and astronautics. The Motion simulation table can simulate all kinds of attitude of the spacecraft in real flight and reproduce the dynamic characteristics of the flight control system. The performance of the guidance system, control system and the corresponding devices on the aircraft tested repeatedly. After collecting test data, redesign and improve it to meet the performance requirements of the overall design of the aircraft.

Testing Simulator performance always linked to the reliability and confidence of simulation and test trials is the base for aviation accuracy and performance of aerospace products. As the rapid development of inertial navigation systems [1-3], the research and manufacturing of inertial guidance test equipment becomes an important issue [4]. One of the most important inertial guidance test equipment is a flight motion simulator [5-6]. Therefore, Motion simulator control research has important significance in the aviation, Aerospace and national defense.

The ZPETC approach has gained attention by numerous researchers [5-7]. The ZPETC approach delivers the overall tracking system with zero phase error characteristics and rules out the phase error that affected by NMP and has unity gain for low frequencies [8-13].

ISSN: 2005-4297 IJCA

In this article, studied the application of feed forward compensation in the servo motor control based Motion table control system. In view of the imperfections of some previous compensation ZPETC approach, discussed here an improved design method with feed forward compensation. The signal lead value cannot be received during the cognitive process in the motion simulator turntable system using ZPETC approximation. Pointing at the shortcomings caused by the approximation, this article gives an improvement ZPETC approximate design based on the premises that the system has zero phase error feedforward compensation. It makes the frequency characteristic of the system in a wide range, the gain of approximately is one and the phase shift is approximately zero. More significantly, this improved method does not require an advanced value for the given instruction signal.

2. Establishment of Motion Simulator Turntable Model and Parameter Selection

Turret azimuth axis based Motion simulation table control is a complex function of the shaft, which controls typical structure. This article will primarily consider the axis control strategy. Various control system control strategies studied before to obtain the mathematical model of the system. This article following the kinetic equation, application-modeling mechanism.

Servo system design starts with the selection of the motor. To overcome the load of the controlled system, the motor must overcome the friction torque of the motor itself and the inertial torque of the motor rotor. In electric servo actuator, the DC motor is the best. In this paper, DC motor load structure mathematical model utilized as indicated in Figure (1).

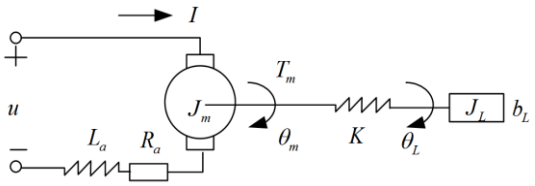

Figure 1. Motor-Load Model

Parameters of the specified motor is as defined below:

$u(t)$ -Motor armature voltage (V); R_a -Motor armature resistance (Ω); L_a -Motor armature inductance (H);

I -Flow armature(A); J_m -Moment of inertia of the rotor($kg \cdot m^2$); J_a -Moment of inertia of the shaft ($kg \cdot m^2$); J_L - Moment of inertia ($kg \cdot m^2$); θ_m - Torque motor rotor angle (rad); θ_L - Frame and axle load angle (rad); b_L - Motor, drive shaft, the load frame viscous friction coefficient (N · m / rad / s); T_L - End load output torque (N · m); T_m - Torque motor electromagnetic torque (N · m); K_i - DC torque motor torque coefficient (N · m / A); K_e - DC torque motor back EMF coefficient (V / rad / s); E - DC torque motor back EMF (V); K- Shaft stiffness factor.

Due to the extended shaft, mass distribution over the length of the shaft, so its inertia is negligible.

Firstly, the equation of DC torque motor armature circuit is

$$u = E + IR_a + L_a \frac{dI}{dt} = K_e \dot{\theta}_m + IR_a + L_a \frac{dI}{dt} \tag{1}$$

Armature current is proportional to the motor torque

$$/T_m = K_i I \tag{2}$$

For torque motor with load, the friction load, the kinetic equation is

$$T_m = J_m \frac{d\omega_m}{dt} + b_l \omega_m + K(\theta_m - \theta)\sum \tag{3}$$

Where $\omega_m = \frac{d\theta_m}{dt}$

Then on the load side of differential equation analysis

$$J_L \frac{d\omega_L}{dt} = T_L - b_L \omega_L \tag{4}$$

Theoretically, The Hook's law can obtain

$$K(\theta_m - \theta_L) = T_L \tag{5}$$

Where the angular velocity of the load side

$$\omega_L = \frac{d\theta_L}{dt} \tag{6}$$

By using the equations from (1) to (6), the following model structure obtained as shown in Figure (2).

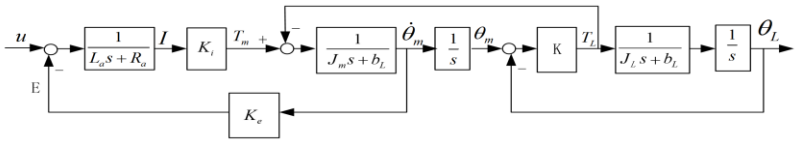

Figure 2. Motor-Load Model Block Diagram

Generally, when the shaft rigidity is large, *i.e.* stiffness coefficient K is infinite, θ_m and θ_L Oscillation link between the degradation 1. In general, armature inductance, motor torque and viscosity coefficient are very small. Moreover, it can be approximately zero.

Make

$$J = J_m + J_L \tag{7}$$

$$\theta = \theta_m = \theta_L \tag{8}$$

At the same time sort the total resistance of the motor shaft load torque T_f, then motor load model would be as follows

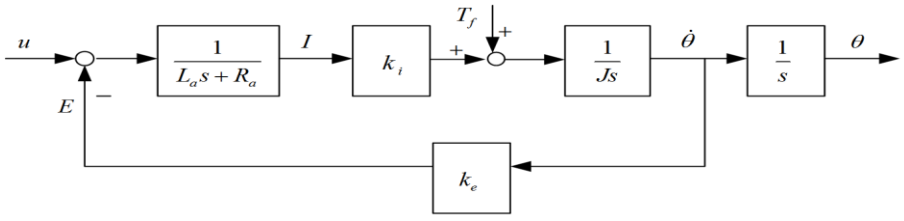

Figure 3. Ideal Motor-Load Model Block Diagram

From Figure (3). u To θ, The transfer function is

$$\frac{\theta(s)}{u(s)} = \frac{K_i}{(L_a s + R_a)Js + K_i K_e} \tag{9}$$

From equation (9), it is clear that the servo system is a standard second-order system. In this paper, 250LYX135 type torque motor is used. The main characteristics of the motor system are:

Stall peak voltage: $U_{fd} = 135$ V; Peak Stall Current: $I_{fd} = 30$ A;

Peak Stall Torque: $T_{fd} = 450$ N.m; Maximum load speed: $n_0 = 100$ r / min;

Inductance: $L = 50$ mH; Motor potential factor: $K_e = \frac{9.55 \times U_d}{n_0} = 123.18$ V.S / rad

Motor torque constant: $K_t = \frac{T_{fd}}{I_{fd}} = \frac{340}{17.5}$ =19.43N.m/A; Torque motor armature resistance: $R_a = \frac{U_{fd}}{I_{fd}} = \frac{110}{17.5}$ =6.29 Ω; Total motor shaft moment of inertia: $J = 5$ kg.m2

The total resistance of the motor shaft load torque range: $T_f = 4.5 \sim 9$ N.m

Actual servo systems are generally more complex and difficult to model accurately that reflects the characteristics of the system. To facilitate debugging of the actual system, typically control system with simplified mechanism combined using another modeling method based on the frequency characteristics of the system.

2.1. Multi Loop Control System for Motion Simulation Table Control

In essence, flight Motion simulation table control is a high precision position and speed servo system.

For motion simulation control system, the driving element electric motor. Essentially closed-loop system is the position or speed of a motor. Negative feedback uses to reduce the sensitivity of the system. At the same time, a series of control devices linked in series to make a closed loop. This structural pattern is prosperous in order to bring down the sensitivity of the system to alter the parameters of the motor.

The motor control scheme planned as a "three ring" structure, which is the current loop, speed loop and position loop. The character of current and velocity loop is to increase the stiffness of the scheme to suppress the nonlinearities and external disturbance of the system. The precision of the control scheme ensured by the position loop. A wide variety of control algorithms implemented in the position loop by digital means.

In this article, Motion simulation table control is a typical three closed loop control structure.

2.2. Current Loop Structure

The following are just a summary of each closed-loop designs.

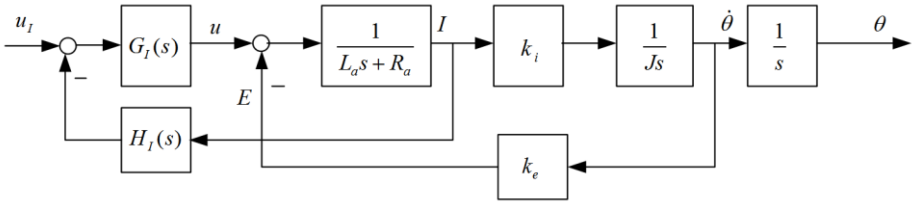

Figure 4. Current Loop Structure

In Figure (4), $G_I(s)$ PI Control structure and $H_I(s)$ is the current feedback factor.

2.3. Speed Loop Structure

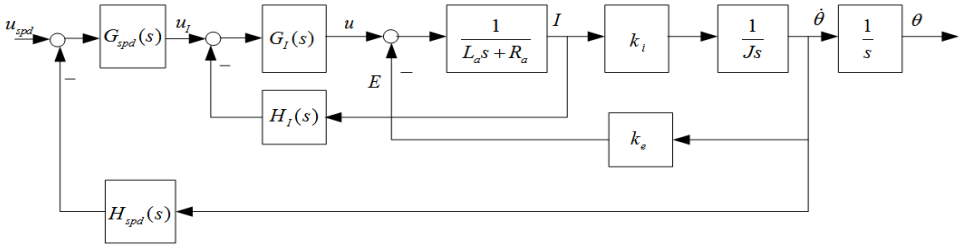

Figure 5. Speed Loop Structure

In Figure (5), feedback link $H_{spd}(s)$ used in order to reduce the impact of noise interference. Speed regulator $G_{spd}(s)$ is General design PI control link. Velocity feedback could suppress the negative influence of the inter-axis coupling torque and of mechanical friction.

2.4. Position Loop Structure

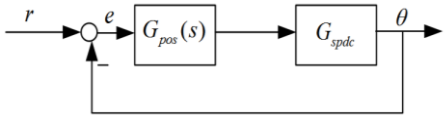

Figure 6. Position Loop Structure

In Figure (6) $G_{spdc}(s)$ is the transfer function block diagram as shown in Figure (5), and $G_{pos}(s)$ is position regulator .The transfer function of the control part is designed in the continuous domain but converted to discrete to use in it practically.

3. Design ZPETC

The servo system speed closed-loop transfer function $G_{cspd}(s)$, the design of ZPETC can be $\frac{G_{cspd}(s)}{s}$

1. For the discrete system, select the sampling period is $1\,ms$:

$$G(z^{-1}) = Z(ZOH \cdot \frac{G_{cspd}(s)}{s}) = \frac{z^{-d} B_c^a(z^{-1}) B_c^u(z^{-1})}{A_c(z^{-1})} = \frac{3.974\times10^{-5}(z+0.0052)(z+1.1795)}{z^3 - 1.915z^2 + 0.915z - 7.622\times10^{-9}}$$
$$= \frac{z^{-1}3.974\times10^{-5}(1+0.0052z^{-1})(1+1.1795z^{-1})}{1-1.915z^{-1}+0.915z^{-2}-7.622\times10^{-9}z^{-3}} \quad (10)$$

2. The following can be designed using ZPETC:

$$G_f(z^{-1}) = ZPETC(G(z^{-1})) = \frac{z^d A_c(z^{-1}) B_c^u(z)}{B_c^a(z^{-1})\left[B_c^u(1)\right]^2}$$
$$= \frac{z(1-1.915z^{-1}+0.915z^{-2}-7.622\times10^{-9}z^{-3})(1+1.1795z)}{3.974\times10^{-5}(1+0.0052z^{-1})\left[1+1.1795\right]^2}$$
$$= \frac{5297.3z^2(1.1795-1.2587z^{-1}-0.8358z^{-2}+0.9149z^{-3}-7.622\times10^{-7}z^{-4})}{(1+0.0052z^{-1})} \quad (11)$$

ZPETC transfer function:

$$G_f(z^{-1})G(z^{-1}) = \frac{(1+1.1795z^{-1})(1+1.1795z)}{4.7502} \quad (12)$$

This is the ideal situation and in the whole frequency domain, phase shift is zero and the low frequency amplitude difference is zero.

3. Approximate design

Consider step 2, according to the design $G_f(z^{-1})$, The output of the feedforward compensation is expressed as:

$$r_f(k) = 5297.3*(1.1795r(k+2)-1.2587r(k+1)-0.8358r(k)+0.9149r(k-1)$$
$$-7.622\times10^{-7}r(k-2))-0.0052r_f(k-1) \quad (13)$$

According to previous analysis, ZPETC design given instruction that requires two steps ahead of the value in steps of 1^{ms}. For Practical application two steps ahead value is ignored, obtain the following compensation components:

$$G_f(z^{-1}) = \frac{5297.3(1.1795-1.2587z^{-1}-0.8358z^{-2}+0.9149z^{-3}-7.622\times10^{-7}z^{-4})}{(1+0.0052z^{-1})} \quad (14)$$

Output can be compared to the compensation link:

$$r_f(k) = 5297.3*(1.1795r(k)-1.2587r(k-1)-0.8358r(k-2)+0.9149r(k-3)$$
$$-7.622\times10^{-7}r(k-4))-0.0052r_f(k-1) \quad (15)$$

It can be seen that this compensation step no longer requires the advance value of the given command signal.

3.1. The Simulation Results with ZPETC and Approximate ZPETC

Approximate ZPETC applied to servo system to simulate the response curve, dotted line shows the command signal and Solid line is the output.

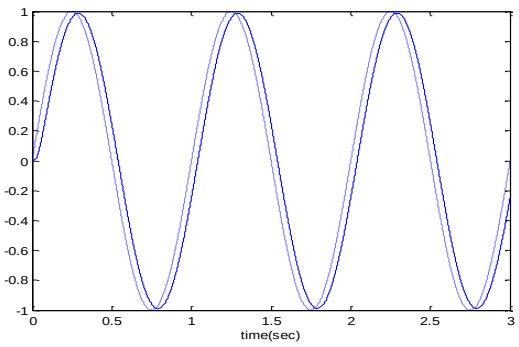

Figure 7. 1Hz Sine Wave (Uncompensated)

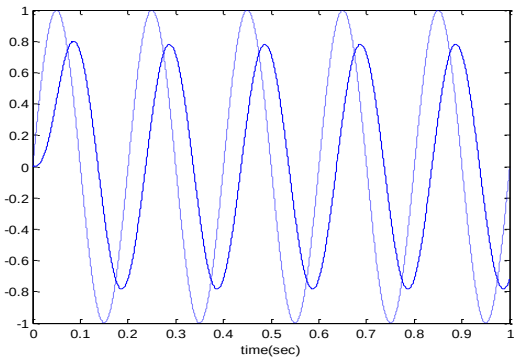

Figure 8. 5Hz Sine Wave (Uncompensated)

After the system was added approximate ZPETC, the response curve of the system shown in figure below

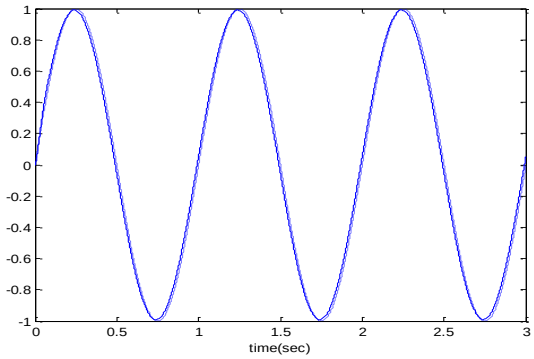

Figure 9. 1Hz Sine Wave (Compensated)

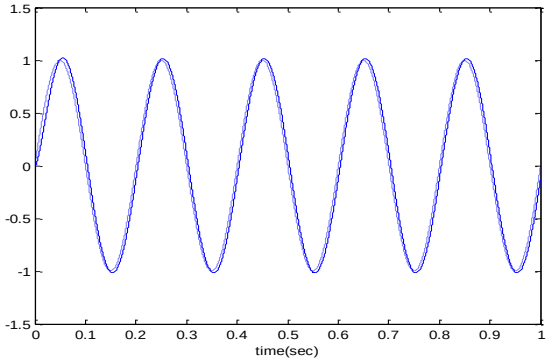

Figure 10. 5Hz Sine Wave (Compensated)

It is clear from the above figure, tracking system performance significantly improved.

However, since the application process, ignoring the several steps ahead value in approximate ZPETC. When the sampling period is 1^{ms}, $d+s=2$ and When given instruction signal frequency exceeds 14Hz, the tracking phase lag of more than 10 degrees, do not achieve the tracking performance. Therefore, the following result verifies that this approximation method limits the servo system to broaden the bandwidth of the system.

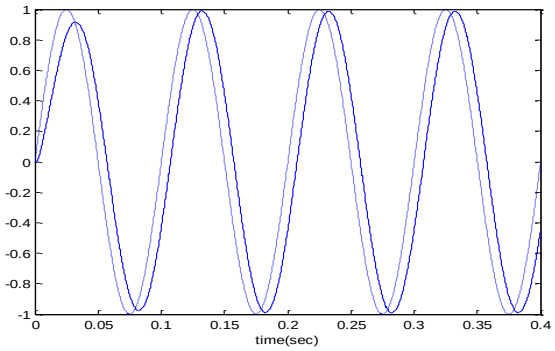

Figure 11. 10Hz Sine Wave (Compensated)

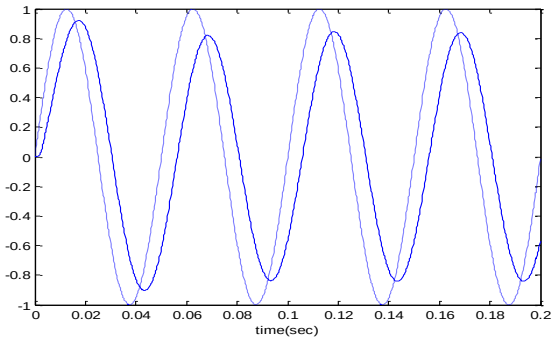

Figure 12. 20Hz Sine Wave (Compensated)

4. Improved Zero Phase Error Feed Forward Compensation

Due to use of the advance value for the feedforward compensation in the approximate ZPETC, the ZPETC of the approximate design has a drawback. This paper presents an improved method for designing ZPETC. The improved feedforward compensation method does not require an advanced value for the feedforward compensation. The phase shift of the system after correction is approximately zero in a large frequency band and the gain is approximately one.

4.1. Considering Minimum Phase Systems

First, consider the simplest case: the closed-loop system for minimum phase $G_m(s)$, Design feed forward compensator $G_{mf}(s) = \frac{1}{G_m(s)}$, assuming that the actual practice, ignore m Step instructions advance value.

For feed-forward compensation, assuming the transfer function $G_m'(s) = e^{-\tau s} G_m(s)$ part of a feedforward compensation

$$G_{mf}'(s) = \frac{1}{G_m'(s)} = \frac{e^{\tau s}}{G_m(s)} \tag{16}$$

Based on the above situation, it is easy to get to meet the actual needs of the system compensator. Meanwhile the compensator does not require advance instruction signal values. Detailed analysis of non-minimum system is given in next section.

4.2. Non-Minimum Phase System

For the following non-minimum phase system:

$$G_c(z^{-1}) = \frac{z^{-d}B_c(z^{-1})}{A_c(z^{-1})} = \frac{z^{-d}B_c^a(z^{-1})B_c^u(z^{-1})}{A_c(z^{-1})} \tag{17}$$

Zero phase feedforward compensation controller:

$$e^{-\tau s}\cdot G_c(s) \quad G_{cf}(z^{-1}) = ZPETC(G_c(z^{-1})) = \frac{z^d A_c(z^{-1})B_c^u(z)}{B_c^a(z^{-1})[B_c^u(1)]^2} \tag{18}$$

For the Actual use of the advance value, we ignore step $d+s$:

$$G_{cf}'(z^{-1}) = z^{-d-s}G_{cf}(z^{-1}) = z^{-d-s}\frac{z^d A_c(z^{-1})B_c^u(z)}{B_c^a(z^{-1})[B_c^u(1)]^2} = \frac{z^{-s}A_c(z^{-1})B_c^u(z)}{B_c^a(z^{-1})[B_c^u(1)]^2} \tag{19}$$

4.3. Pade Approximation

In the actual design process, we first need to consider the lag $e^{-\tau s}$ link pade approximately $R_{r,r}(s)$: [21]

$$e^{-\tau s} \approx R_{r,r}(s) = \frac{N_r(\tau s)}{D_r(\tau s)} \tag{20}$$

the formula (20) is converted to the following equation :

$$R_{2,2}(s) = \frac{s^2 - \frac{6}{\tau}s + \frac{12}{\tau^2}}{s^2 + \frac{6}{\tau}s + \frac{12}{\tau^2}} \tag{21}$$

Design of Improved Zero Phase Difference Feedforward Compensation

$R_{2,2}(s)$ Z-transform is $R_{2,2}(z^{-1})$:

$$R_{2,2}(z^{-1}) = \frac{z^{-d_r}B_r^u(z^{-1})B_r^a(z^{-1})}{A_r(z^{-1})} \tag{22}$$

Some calculations are not included because shortage of space. The transfer function of the whole system after using the compensation link can be obtained

$$\begin{aligned} G_f(z^{-1})\cdot G_c(z^{-1}) &= z^{-d-s-d_r-s_r}\cdot G_{cf}(z^{-1})\cdot G_{rf}(z^{-1})\cdot G_c(z^{-1}) \\ &= z^{-d-s-d_r-s_r}\cdot\frac{z^d A_c(z^{-1})B_c^u(z)}{B_c^a(z^{-1})[B_c^u(1)]^2}\cdot\frac{z^{d_r}A_r(z^{-1})B_r^u(z)}{B_r^a(z^{-1})[B_r^u(1)]^2}\cdot\frac{B_c^a(z^{-1})B_c^u(z^{-1})}{A_c(z^{-1})} \\ &= z^{-d-s-d_r-s_r}\cdot\frac{B_c^a(z^{-1})B_c^u(z)}{[B_c^u(1)]^2}\cdot\frac{z^{d_r}A_r(z^{-1})B_r^u(z)}{B_r^a(z^{-1})[B_r^u(1)]^2} \end{aligned} \tag{23}$$

4.4. Improved ZPETC Design for Motion Simulator Turntable System

According to the iterative algorithm $\tau = 4T$, the following improved ZPETC is designed.

e^{-4Ts} Second-order pade approximation Z is converted into:

$$R_{2,2}(z^{-1}) = \frac{0.4 - 0.2z^{-1} + z^{-2}}{1 - 0.2z^{-1} + 0.4z^{-2}} \tag{24}$$

According to $R_{2,2}(Z^{-1})$ ZPETC designed to:

$$ZPETC(R_{2,2}(z^{-1})) = \frac{z^2(1-0.2z^{-1}+0.4z^{-2})(0.4z^{-2}-0.2z^{-1}+1)}{1.414} \tag{25}$$

Therefore, the improved ZPETC system transfer function becomes:

$$\begin{aligned} G_f(z^{-1}) &= z^{-4}ZPETC(R_{2,2}(z^{-1})G_{c1}(z^{-1})) \\ &= \frac{5297.3(1.1795-1.2587z^{-1}-0.8358z^{-2}+0.9149z^{-3}-7.622\times10^{-7}z^{-4})(1-0.2z^{-1}+0.4z^{-2})^2}{1.414(1+0.0052z^{-1})} \end{aligned} \tag{26}$$

Moreover, the output of the compensation link is:

$$\begin{aligned} r_f(k) = &\frac{5297.3}{1.414}*(0.4718r(k)-0.8337r(k-1)+1.4335r(k-2)-1.2407r(k-3) \\ &-0.4349r(k-4)+0.8284r(k-5)-0.5905r(k-6)+0.3660r(k-7))-0.0052r_f(k-1) \end{aligned} \tag{27}$$

5. Experimental Results

In order to obtain each frequency characteristic, a direct link to the feed-forward compensation applied before the position closed loop configuration. When designing the feed forward compensation to obtain the position of the closed-loop transfer function of the frequency point fit $G_{pos}(s)$, the transfer function designed to compensate links. Due to limitations of the motor performance, frequency characteristics of the motion simulation turntable obtained within range from 1Hz to 10Hz.

For a given position command signal $\theta(t) = A\sin(\omega t) = A\sin(2\pi ft)$,

The angular velocity $\dot{\theta}(t) = A\omega\cos(\omega t) = 2\pi fA\cos(2\pi ft)$,

Angular acceleration is $\ddot{\theta}(t) = -A\omega^2\cos(\omega t) = -(2\pi f)^2 A\cos(2\pi ft)$.

The maximum angular velocity and the maximum angular acceleration are as follows:

$\dot{\theta}_{\max} = A(2\pi f)$, $\ddot{\theta}_{\max} = A(2\pi f)^2$.

Due to limitations of the motor performance, maximum acceleration can only reach about 1500°/s^2 ~ 2000°/s^2. With the increase of frequency, the maximum amplitude of the given command will reduced. When frequency is more than 10Hz, the amplitude is very small and the angular position accuracy is not satisfied. Therefore, it is difficult to guarantee the accuracy of the points above 10HZ.

Sinusoidal response process collecting data points before and after the compensation system during the simulation in MATLAB. Prior to compensate for actual servo system 1Hz ~ 10Hz measured response waveform shown figure below.

Uncompensated system with 1Hz waveform response are given below

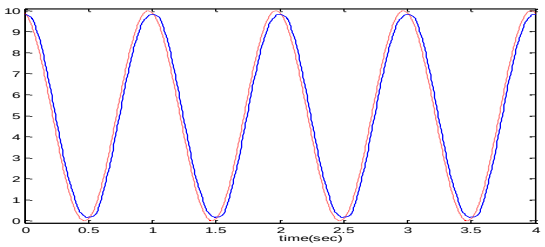

Figure 13. 1Hz Sine Wave (Uncompensated)

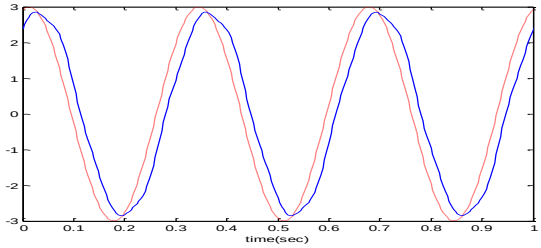

Figure 14. 3Hz Sine Wave (Uncompensated)

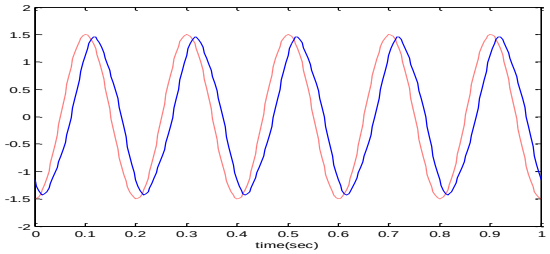

Figure 15. 5Hz Sine Wave (Uncompensated)

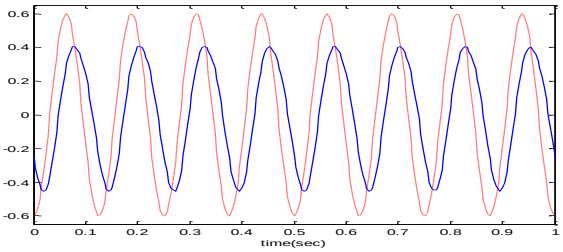

Figure 16. 8Hz Sine Wave (Uncompensated)

After adding the compensation, the system response waveform shown in Figure below

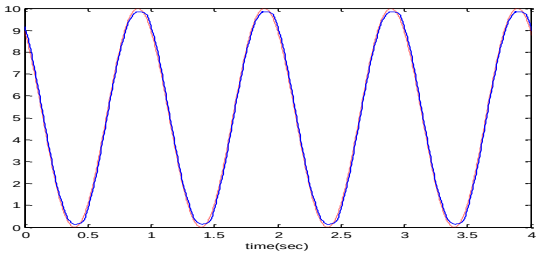

Figure 17. Compensated with 1Hz Response

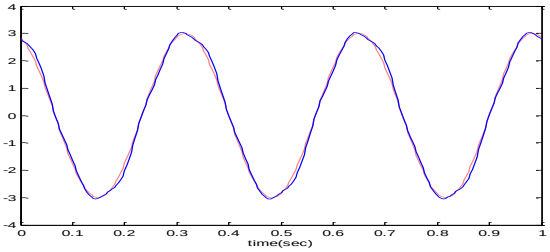

Figure 18. Compensated with 3Hz Response

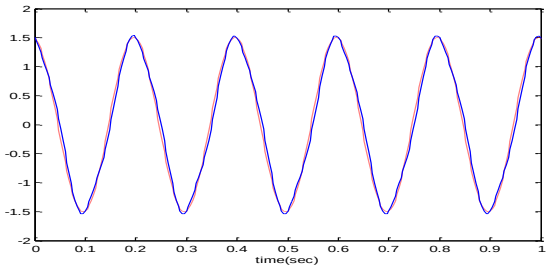

Figure 19. Compensated with 5Hz Response

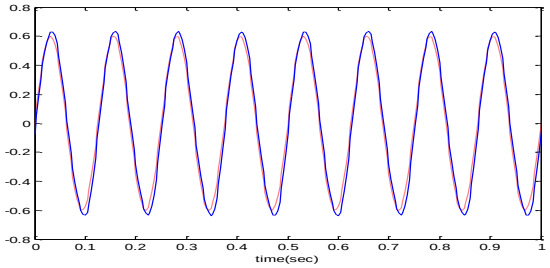

Figure 20. Compensated with 8Hz Response

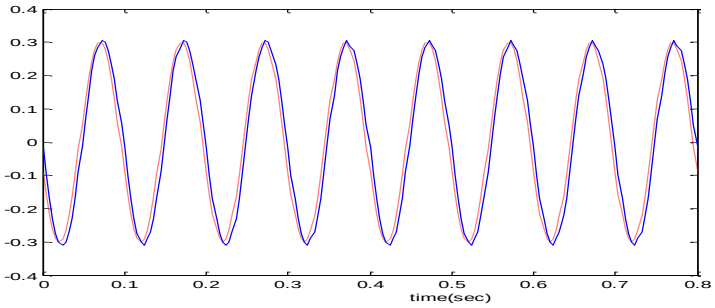

Figure 21. Compensated with 10Hz Response

It is clear from the above result that the frequency bandwidth has broadened, and frequency characteristics of the system measured within the range of 10Hz because of the limitations of the motor performance. Therefore, the system frequency can further widened, but the correct motor system selection is very important.

The method-improved design ZPETC added to the original position before the closed-loop system to compensate. Design $\tau = 4T$.

The following table shows the comparison of the original system, approximate ZPETC compensation and improvements ZPETC compensation measured within 10HZ.

Table 3.1. Comparison Analysis of Compensation Effect

	The original system		Approximate ZPETC compensation		Improved compensation ZPETC	
frequency	Spread	difference	Spread	difference	Spread	difference
1	0.98	-9.19	1.01	-0.88	1.00	0.95
2	0.98	-14.53	1.00	-1.64	1.01	1.98
3	0.97	-19.44	1.03	-0.17	1.05	4.83
4	0.90	-26.31	1.06	-0.67	1.06	5.61
5	0.95	-31.18	1.03	-5.98	1.06	2.01
6	0.86	-40.37	0.97	-8.78	1.07	0.37
6.5	0.87	-41.17	1.02	-7.84	1.08	1.70
7	0.67	-52.14	0.95	-9.00	1.08	0.16
8	0.56	-54.36	1.01	-8.24	1.09	0.43
9	0.71	-57.13	0.94	-7.48	1.09	-1.08
10	0.42	-64.8	0.96	-7.41	1.14	-2.16

It is clear that the improved method further improves the phase difference, but a slight gap in the area of difference, as the frequency increases, the amplitude difference increases.

However, has observed that there are problems in the real time application. The accuracy of the system model in the design process has great influence on the design of the compensation link. With a discrete model, zero-order hold should use with the system. If the computational precision in the discrete process is too low, it will also affect the design part of the compensation. Although the phase is well compensated, but the amplitude problem needs to study further in real time application.

6. Conclusion

In this article, improved zero phase error tracking controller (ZPETC) approach is introduced to overcome NMP zero problem with application to motion simulator table. The basic components of the servo based load model system are established. Approximate ZPETC and improved ZPETC methods successfully applied to the motion simulation table and simulated. The test results compared and analyzed. Experimental results verify that Improved approximation ZPETC broaden the bandwidth of the system and satisfy the required performance of the system. The simulation results of the proposed algorithm satisfy the overall tracking performance of the motion simulation turntable.

Acknowledgment

This study is supported by the College of Automation Engineering, Nanjing University of Aeronautics and Astronautics Nanjing, China and is funded by “National Natural Science Foundation of China (NSFC)” under grand No. 61503185.

References

[1] J. F. Vasconcelos, C. Silvestre, P. Oliveira and B. Guerreiro, “Embedded UAV model and LASER aiding techniques for inertial navigation systems”, Control Engineering Practice, vol. 18, no. 3, **(2010)**, pp. 262-278.
[2] M. S. Grewal, A. P. Andrews and C. G. Bartone, “Global navigation satellite systems, inertial navigation, and integration”, John Wiley & Sons, **(2013)**.
[3] L. Zhang, H. Yang, S. Zhang, H. Cai and S. Qian, “Strapdown stellar-inertial guidance system for launch vehicle”, Aerospace Science and Technology, vol. 33, no. 1, **(2014)**, pp. 122-134.
[4] P. G. Savage, “Blazing gyros: The evolution of strapdown inertial navigation technology for aircraft”, Journal of Guidance, Control, and Dynamics, vol. 36, no. 3, **(2013)**, pp. 637-655.

[5] K. Klumper, A. Morbi, K. J. Chisholm, R. Beranek, M. Ahmadi and R. Langlois, "Orientation control of Atlas: A novel motion simulation platform", Mechatronics, vol. 22, no. 8, **(2012)**, pp. 1112-1123.
[6] G. Zhifu, C. Jian and Z. Keding, "Design and experiments of model-free compound controller of flight simulator", Chinese Journal of Aeronautics, vol. 22, no. 6, **(2009)**, pp. 644-648.
[7] N. Ishak, M. Tajjudin, H. Ismail, M. Hezri Fazalul Rahiman, Y. Md Sam and R. Adnan, "Tracking control for electro-hydraulic actuator using ZPETC", In Control and System Graduate Research Colloquium (ICSGRC), IEEE, **(2011)**, pp. 94-97.
[8] H. Ismail, N. Ishak, M. Tajjudin, M. Hezri Fazalul Rahiman and R. Adnan, "Positioning and Tracking Control of an XY table", In Control System, Computing and Engineering (ICCSCE), 2011 IEEE International Conference on IEEE, **(2011)**, pp. 343-347.
[9] R. Adnan, A. Manan Samad, N. Md Tahir, M. Hezri Fazalul Rahiman and M. Marzuki Mustafa, "Trajectory zero phase error tracking control using comparing coefficients method", In Signal Processing & Its Applications, CSPA 2009. 5th International Colloquium on IEEE, **(2009)**, pp. 385-390.
[10] R. Adnan, A. Manan Samad and M. Marzuki Mustafa, "Real-time control of non-minimum phase electro-hydraulic system using trajectory-adaptive ZPETC", In Signal Processing and its Applications (CSPA), 2011 IEEE 7th International Colloquium on IEEE, **(2011)**, pp. 72-76.
[11] M. Marzuki Mustafa, "Trajectory-adaptive digital tracking controllers for non-minimum phase systems without factorisation of zeros", IEE Proceedings-Control Theory and Applications, vol. 149, no. 2, **(2002)**, pp. 157-162.
[12] M. Pal, G. Sarkar, R. Kumar Barai and T. Roy, "Reference input tracking of inversion-based non-minimum phase system using adaptive two-degree-of-freedom control", In 2016 IEEE First International Conference on Control, Measurement and Instrumentation (CMI), IEEE, **(2016)**, pp. 5080-513.
[13] K. S. Ramani, M. Duan, C. E. Okwudire and A. Galip Ulsoy, "Tracking Control of Linear Time-Invariant Non minimum Phase Systems Using Filtered Basis Functions", Journal of Dynamic Systems, Measurement, and Control, vol. 139, no. 1, **(2017)**, 011001.
[14] G. J. Silva, A. B. S. P. Datta and S. P. Bhattacharyya, "Controller design via Pade approximation can lead to instability", In Decision and Control, Proceedings of the 40th IEEE Conference on IEEE, vol. 5, **(2001)**, pp. 4733-4737.

